International RILEM Conference on Materials, Systems and Structures in Civil Engineering
Conference segment on Moisture in Materials and Structures
22-24 August 2016, Technical University of Denmark, Lyngby, Denmark

NUMERICAL SIMULATION OF HUMIDITY FIELDS IN CONCRETE CONSIDERING THE MODEL CODE FORMULATION

Mateus Oliveira [(1)], Miguel Azenha[(1)], Paulo B. Lourenço [(1)]

[(1)] ISISE, University of Minho

Abstract
The influence of moisture content in the behavior and performance of construction materials, such as concrete is well identified in the literature. For concrete structures, the humidity content is influenced by the processes of drying and self-desiccation that should be reasonably predicted in design stages for several reasons. This work focuses on the formulation for the relative humidity field presented in Model Codes 1990/2010, and provides an evaluation of its feasibility in view of existing data in the literature. This adoption was done because of the relative simplicity of the modelling and the comprehensiveness of the Model Code itself. Considering this formulation, an implementation was made through the use of the finite difference method. The implemented model was used for simulation of experimental results from two references in which relative humidity profiles were measured. In general terms, the model could fairly fit the experimental results, in spite of the need to specifically address the proposal of a boundary transfer coefficient to achieve successful simulations.

1. Introduction

The moisture content has significative influence in the behavior and performance of construction materials, such as concrete [1-3]. The influence of moisture on concrete mechanical aspects and response was studied by different authors [4, 5]. Furthermore, humidity states have influence in the durability of concrete structures, particularly by interaction with the carbon dioxide diffusion and the carbonation processes [6-9], as well as with the chloride ingress process [10] and with other multi-physics processes, such as the ingress of sulfates into concrete [11]. Therefore, the knowledge of the moisture distribution within concrete, since the construction and throughout the service life, may be considered very important.
The movement of water/moisture in porous media such as concrete or mortar is a complex matter, because cementitious materials are known to have a wide range of diameters in their pore structure, spanning from radiuses as small as 10^{-10} m (gel pores), to radiuses up to 10^{-2} m (air voids/capillary pores) [12]. This complex structure of pores, and associated connectivity network, are randomly distributed [13].
Even though many approaches have been forwarded for the simulation of moisture/humidity fields in concrete, considering several potential field variable (e.g. absolute water, vapour

pressure, relative humidity), the present work is centered on the approach of considering relative humidity as the field variable. Baroghel-Bouny *et al.* [4] define internal relative humidity of concrete as the relative humidity *(h)* of the gaseous phase in equilibrium with the interstitial liquid phase in the pore network of the material.
In terms of modeling, Bažant and Najjar [14] used a numerical formulation based on internal concrete humidity as the driving potential for moisture movements. It embraced a specific model for the corresponding diffusivity coefficient D_h. This approach has been adopted by Model Code 1990 [15] and Model Code 2010 [16]. The corresponding field equation is presented in Eq. 1, where *t* stands for time.

$$\frac{\partial h}{\partial t} = div\, D_h \left(grad\left(h\right)\right) \qquad \text{Eq. 1}$$

For the diffusion coefficient in isothermal conditions, it can be expressed as a function of the pore relative humidity $0 < h < 1$ [14-16]:

$$D_h = D_1 \left[\alpha + \frac{1-\alpha}{1+\left[\left(1-h\right) / \left(1-h_c\right)^n \right]} \right] \qquad \text{Eq. 2}$$

where: D_1 is the maximum value of D_h for $h = 1$ [m^2/s]; D_0 is the minimum D_h for $h = 0$ [m^2/s],
$\alpha = D_0 / D_1 = 0.05$, h_c the relative pore humidity at $D_h\left(h\right) = 0.5 D_1$ ($h_c = 0.80$) and n is an exponent ($n=15$). According to MC1990 and MC2010, D_1 is defined as a function of the mean compressive strength of concrete f_{cm} expressed in MPa as:

$$D_1 = \frac{D_{1,0}}{f_{cm} - 8} \qquad D_{1,0} = 1 \times 10^{-8}\, m^2 / s \;\; or \;\; D_{1,0} = 864\, mm^2 / day \qquad \text{Eq. 3}$$

It is worth to remark that neither MC1990 nor MC2010 [15, 16] afford recommendations on how boundary conditions should be modeled, however it can have an important influence on the results [1, 17]. This paper focuses in the application of the humidity modelling approach of MC1990/2010 to the experiments reported by Persson [18] and Kim and Lee [19], in which humidity measurements at several depths were performed during the process of drying. After the present introduction, Section 2 focuses on the axisymmetric implementation through the finite difference method, whereas the simulations and discussions are held in Section 3. The conclusions of the work are then forwarded in Section 4.

2. Algorithm in axisymmetric conditions

In the present section, the formulation of the humidity field in axisymmetric conditions is presented. For axisymmetric conditions the grid that corresponds to the simulation domain is shown in Figure 1. Two directions are defined: the angular θ and the radial p. In the radial direction each node has a distance Δp from the neighboring one. The derivation presented herein assumes three consecutive nodes positioned for along the angular discretization,

termed as *θ-1, θ*, and *θ+1*. In the radial direction, three points are also considered: *i-1*, *i* and *i+1*. Each point is identified with two indexes that characterize its position in the set of points of the grid: $p^{i,\theta}$ as shown in Figure 1.

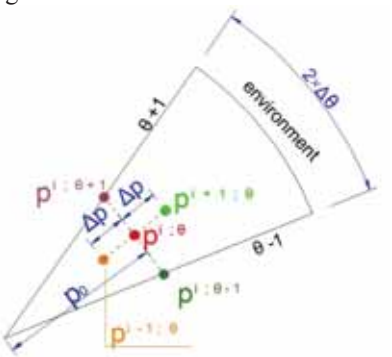

Figure 1. Axisymmetric condition for FDM (adapted from Croft and Lilley [20])

Therefore the general equation for the ∇ and ∇^2 operators for humidity field in axisymmetric conditions can be written as [20]:

$$\nabla h(p,\theta) = \frac{\partial h}{\partial p} + \frac{1}{p}\frac{\partial h}{\partial \theta} \qquad \text{Eq. 4}$$

$$\nabla^2 h(p,\theta) = \frac{\partial h}{\partial p^2} + \frac{1}{p}\frac{\partial h}{\partial p} + \frac{1}{p^2}\frac{\partial^2 h}{\partial \theta^2} \qquad \text{Eq. 5}$$

From Eq. 1, applying the calculus rule, and assuming that the distance between consecutive nodes may be considered small, it may be inferred that small spatial variation of D_h will occur between consecutive nodes. In view of such reasoning, the term $\nabla D_h\left(\frac{\partial h}{\partial p} + \frac{1}{p}\frac{\partial h}{\partial \theta}\right)$ may be disregarded. Consequently, by applying standard finite difference definitions to Eq. 1, while replacing the necessary parameters by equations 4 and 5, one can obtain:

$$\frac{h_{n+1}^{i,\theta} - h_n^{i,\theta}}{\Delta t} = D_h^{i;\theta}\left(\frac{h_{n+1}^{i-1;\theta} - 2h_{n+1}^{i;\theta} + h_{n+1}^{i+1;\theta}}{(\Delta p)^2} + \frac{h_{n+1}^{i-1;\theta} - h_{n+1}^{i+1;\theta}}{2p_0\,\Delta p} + \frac{h_{n+1}^{i;\theta+1} - 2h_{n+1}^{i;\theta} + h_{n+1}^{i;\theta-1}}{(p_0)^2(\Delta\theta)^2}\right) \qquad \text{Eq. 6}$$

Adopting no variation on the angular direction ($\Delta\theta$) due to the axisymmetric condition (Eq. 7), Eq. 8 is obtained as [21]:

$$h_{n+1}^{i;\theta+1} = h_{n+1}^{i;\theta} = h_{n+1}^{i;\theta-1} \qquad \text{Eq. 7}$$

$$\frac{h_{n+1}^{i,\theta}-h_n^{i,\theta}}{\Delta t}=h_{n+1}^{i,\theta}\times\left(1+\frac{2\times D_h^{i;\theta}}{(\Delta p)^2}\right)+h_{n+1}^{i-1;\theta}\times\left(-D_h^{i;\theta}\right)\times\left(\frac{1}{(\Delta p)^2}+\frac{1}{2p_0\,\Delta p}\right)$$
$$+h_{n+1}^{i+1;\theta}\times\left(-D_h^{i;\theta}\right)\times\left(\frac{1}{(\Delta p)^2}-\frac{1}{2p_0\,\Delta p}\right) \quad \text{Eq. 8}$$

For the boundary, the assumption of the Neumann's boundary condition provides [21]:

$$D_h^{i;\theta}\frac{\partial h}{\partial p}=f_{boundary}\left(h_{n+1}^{i,\theta}-h_{env}\right) \quad \text{Eq. 9}$$

Adopting a fictitious node for *"i+1"* and a fictitious humidity $h_{n+1}^{i+1;\theta}$ according to standard finite difference derivations, Eq. 9 may be re-written as:

$$h_{n+1}^{i+1;\theta}=h_{n+1}^{i-1;\theta}+\frac{2\Delta p\times f_{boundary}\times\left(h_{env}-h_{n+1}^{i,\theta}\right)}{D_h^{i;\theta}} \quad \text{Eq. 10}$$

Solving in terms of $h_{n+1}^{i+1;\theta}$ and replacing in Eq. 8, the final equation for the boundary may be expressed as:

$$h_n^{i,\theta}=-h_{env}\times(-2\Delta p)\times(-\Delta t)\times f_{boundary}\times\left(\frac{1}{(\Delta r)^2}+\frac{1}{2p_0\,\Delta r}\right)$$
$$+h_{n+1}^{i-1;\theta}\times\left(2\times\left(-D_h^{i;\theta}\Delta t\right)\times\left(\frac{1}{(\Delta p)^2}\right)\right) \quad \text{Eq. 11}$$

The humidity in each step is calculated in an incremental/iterative process. The *h* value obtained on time step *"n"* is adopted as the first trial value for step *"n+1"*, particularly in regard to the estimation of D_h (implicit backward-Euler formulation). This is a typical nonlinear process, because of the dependence of D_h on *h*. The Newton-Raphson method is used to solve the nonlinear system of equations [22]. The residuals vector was calculated with the difference of humidity values in two consecutives iterations. The convergence criterion was based on the comparison between the norm of the residuals vector with the maximum tolerance, which was assumed equal to 0.0001. More information about the calculation of the residual vector and the overall procedure can be found in Azenha [3] and Oliveira [1]. The axisymmetric implementation was verified with a simple example with the TNO-DIANA® [23].

Additionally to this implementation, a 1D model in non-axysimetric conditions was also derived and deployed. More details about such implementation can be found in Oliveira [1, 2].

3. Simulations

The first group of experiments simulated was tested by Persson [18]. The author casted circular concrete slabs of 1 m diameter and 0.1 m thickness, schematically shown in Figure 2. The specimens were sealed with layers of epoxy resin on their top and bottom flat surfaces [18]. It is remarked that the experiments presented by Persson [18] have been conducted with exposure of concrete to drying at the age of 3 days. Even though the MC1990/2010 approach does not include any specific correction for exposures earlier than 28 days, it was decided to carry out the simulation anyway. This decision was taken because the monitoring depths presented in Persson [18, 24, 25] were the deepest ones found in the literature (max. 35cm deep measurement), thus representing a very unique possibility of validation. Furthermore, the experiments conducted by Kim and Lee [19] with specimens exposed at 3 and 28 days have demonstrated similar results for the largest monitored depths (e.g. 12 cm), thus providing grounds to the simulation attempt reported herein.
Even the environmental conditions during the experiment (temperature and relative humidity) were not constant throughout the entire period of testing, their variation observed by monitoring was limited (for further details see Persson [18]). For such reason the simulation was conducted under the assumption of constant environmental temperature (21ºC) and humidity (33%).
Relative humidity measurements were obtained through cast–in plastic probes placed at depths of 5, 15 and 35 cm from the exposed surface [18, 24, 25] (see Figure 2).

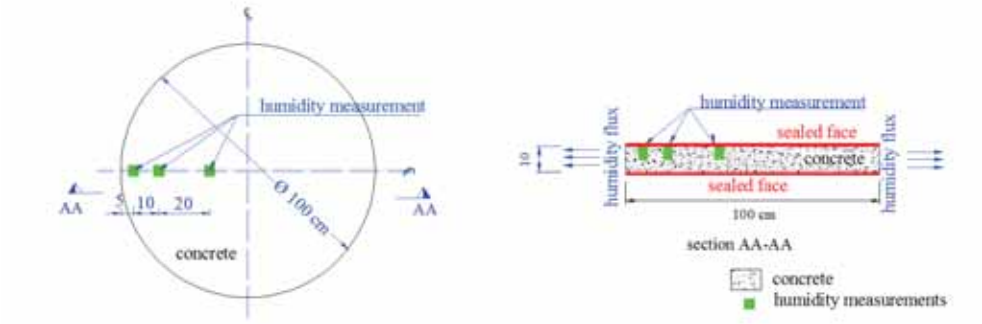

Figure 2. Schematic representation of the geometry and size of test specimens – dimensions in cm (adapted from Persson [24])

Five concrete mixes have been studied, here termed as *Mix 1 and Mix 2, Mix 3, Mix 4* (with silica), *Mix 5* (with silica), with the compositions detailed in Persson [18, 24, 25]. The concrete mixes had average compressive strengths of $f_{cm,\ Mix1}$ = 80 MPa and $f_{cm,\ Mix2}$ = 37 MPa, $f_{cm,\ Mix3}$ = 57 MPa, $f_{cm,\ Mix4}$ = 67 MPa, $f_{cm,\ Mix5}$ = 91 MPa. The effects of self–desiccation were experimentally assessed in sealed specimens and the corresponding humidity decreases were imposed in the numerical simulation, based on the data provided by Persson [24]. Such humidity decreases in the sealed specimens are presented as [day, humidity], for *Mix 1* [28,

0.92; 90, 0.88; 446, 0.86], *Mix 2* [28, 0.96; 90, 0.96; 440, 0.96], *Mix 3* [28, 0.97; 90, 0.95; 446, 0.88], *Mix 4* [28, 0.95; 90, 0.88; 446, 0.83], *Mix 5* [28, 0.88; 90, 0.81; 446, 0.76].
The direct application of the parameters of MC2010 for D_1 ($D_{1,Mix1}$ = 12.2; $D_{1,Mix2}$ = 29.8 mm^2/day; $D_{1,Mix3}$ = 17.6 mm^2/day; $D_{1,Mix4}$ = 14.6 mm^2/day; $D_{1,Mix5}$ = 10.4 mm^2/day) and assumption of Dirichlet boundary conditions (i.e. by imposing the environmental humidity values to the boundary nodes), led to unsatisfactory agreement between numerical results and monitored h (for further details see Oliveira [1]). It was then decided to look for better coherences by making minor changes to the diffusion parameter, whereas inputting a boundary transfer coefficient $f_{boundary}$ to the surface regions. It is remarked that the fitting processes adopted in this work were further performed for an extensive range of values for both D_1 and $f_{boundary}$ parameters, as to evaluate the uniqueness of the initially obtained solution. In fact, D_1 was studied in the range 0.1 mm^2/day to 200 mm^2/day with increments of 0.5 mm^2/day. Simultaneously, $f_{boundary}$ was varied in the range 0.1×10^{-4} m/day to 100×10^{-4} m/day. These ranges considered the recommendations of MC90/2010 and work of Kim and Lee [19] (for further details see Oliveira [1]).
The simulations, for better agreements led to D_1 values that were rather similar to the initial ones (recommended by MC1990/2010): $D_{1,mix1}$ = 12.0 mm^2/day; $D_{1,mix2}$ = 30 mm^2/day, $D_{1,mix3}$ = *8* mm^2/day, $D_{1,mix4}$ = *13* mm^2/day, $D_{1,mix5}$ = *8* mm^2/day, while the fitted values of $f_{boundary}$ for Mix 1, 2, 3, 4 and 5 were respectively 1.4×10^{-4} m/day, 3.0×10^{-4} m/day, 1.0×10^{-4} m/day, 1.5×10^{-4} m/day and 0.8×10^{-4} m/day. To illustrate the quality of the attained coherences for all the simulations, Figure 3 presents both the experimental and simulated results for *Mix1*.

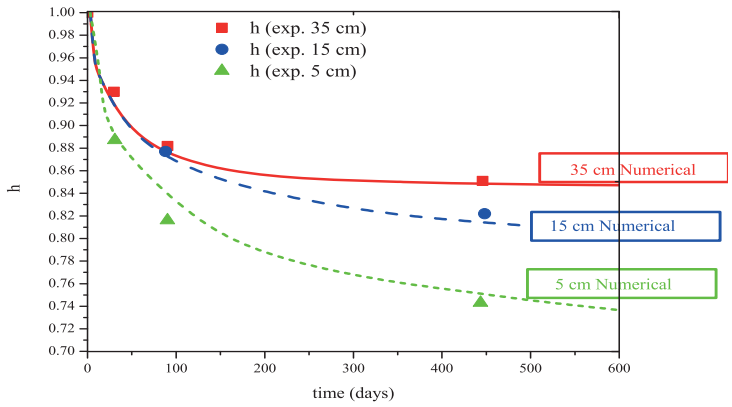

Figure 3. Humidity profiles for *Mix 1*: experimental and numerical results after the fitting process

The second set of simulated experiments was presented by Kim and Lee [19], who studied three different concrete compositions, termed *H*, *M* and *L*, using 10 cm × 10 cm × 20 cm specimens (for concrete the compositions see Kim and Lee [19]). After an initial period in which the specimens were kept inside their mold, they were submerged in water from the age of 1 day until the age of 28 days. At 28 days, the specimens were removed from water, their

surfaces were sealed, and placed in a climatic chamber with $T = 20 \pm 1$ ºC and $h_{env} = 50 \pm 2\%$. The evaporation could only take place through a 10 cm × 10 cm surface, simulating a 1D flux. Humidity sensors were placed at three distinct depths: 3 cm, 7 cm and 12 cm. Kim and Lee [19] also measured the humidity decrease associated to self-desiccation phenomena in companion sealed specimens. At the age of 28 days, the recorded value was stabilized at approximately 95% for mixes *H* and *M*, while the value for mix *L* was ~99%. These values were used as starting conditions for the humidity of concrete in the simulations.

For specimen *M*, the proposed value for D_1 given by the equation presented on the MC2010, used together with Dirichlet boundary conditions, led to relevant discrepancy in regard to the experimental data. A fitting approach for D1 and $f_{boundary}$ was then followed, similarly to the process mentioned above for the data of Persson. The results of the best combination of $f_{boundary}$ and D_1 values for specimen *M* are shown in Figure 4. From the results obtained, it be noticed that a change of D_1 from 16.1mm^2/day to 32 mm^2/day and the introduction of $f_{boundary}$ = 3.2×10^{-4} m/day provided simulation results that approximated the experimental results quite satisfactorily. Similar strategies were taken for specimens *H* and *L*, with the final summary of results for the two sets of experiments being shown in Table 1.

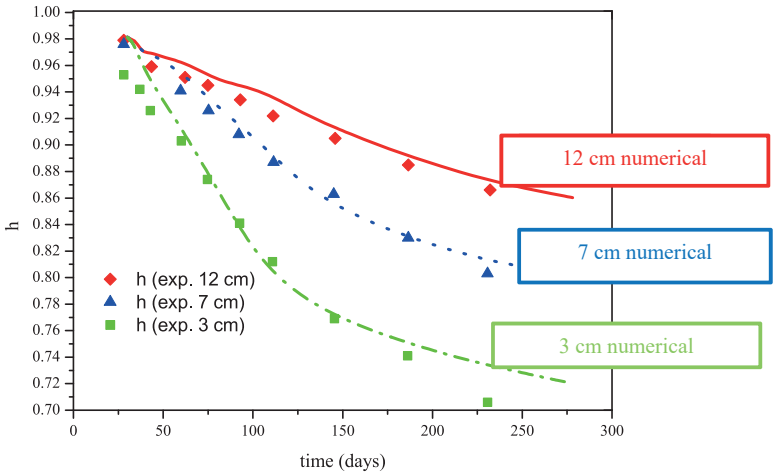

Figure 4 – Humidity profiles specimen *M*: experimental and numerical results after the fitting process

Table 1 Summary of the simulations and results

Designation	f_{cm} (MPa)	D_1 (mm^2/day) MC90/2010	D_1 (mm^2/day) best-fit simulation	$f_{boundary}$ (m/day) (10^{-4}) best-fit simulation
Mix 1	80	12.0	12	1.4
Mix 2	37	29.8	30	3
Mix 3	57	17.6	8	1
Mix 4	67	14.6	13	1.5
Mix 5	91	10.4	8	0.8
H	84	11.4	20	2.0
M	61	16.3	32	3.2
L	30	39.3	52	4.8

Considering the data presented in Table 1, the plot of the attained values of $f_{boundary}$ as function of the compressive strength of the tested concrete is shown in Figure 5, in which a clear tendency can be observed. Indeed, as the compressive strength of concrete increases the boundary transfers are decreasing, in probably in coherence with a less porous boundary. This observation is in agreement with the surface factor theory proposed by Zhi *et al.* [26].
It is remarked that the above relationship solely considers the effect of f_{cm} on $f_{boundary}$, neglecting the potential influence of wind speed on the boundary transfer coefficient. Considering that the present work simulated hardened concrete, this can be considered a plausible interpretation. In this sense, Azenha *et al*. [27, 28] demonstrated experimentally that cementitious based materials exposed to drying process after the ages of 7 days tended to present very low (or even negligible) sensitivity to wind speed in terms of drying velocity (i.e. mass loss).

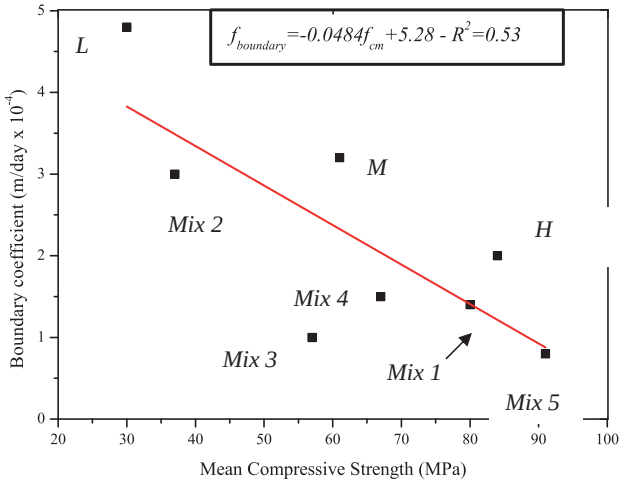

Figure 5 – Correlation between the boundary coefficient and the concrete compressive strength.

4. Conclusions

This paper has presented the application of the MC1990/2010 approach to moisture diffusion simulation to experimental data available in the literature. The implementation of a 1D finite different formulation was presented, and the implemented algorithm was applied to the results of two distinct research works. A total of 8 different mixture compositions and two different specimen sizes were assessed.
It was found that the direct application of the MC1990/2010 approach failed to provide accurate descriptions of the humidity profiles in the tested specimens. However, after a fitting process that included the proposal of a boundary transfer coefficient (as opposed to the imposed humidity at the boundaries that is inferred from the MC1990/2010), it was found that very good predictive accuracies could be reached, with diffusion parameters that resembled

the ones proposed by the Model Codes. It was further found that the proposed boundary coefficients had a clear relationship with the compressive strength of the concrete under consideration.
The validation reported herein can play an important role in assisting design offices and researchers that seek simplified simulation approaches that have proven performance in regard to actual test data.

5. Acknowledgments

The authors acknowledge the funding provided by the program "*Ciência sem Fronteiras*" supported by Brazilian National Council of Technological and Scientific Development (CNPq). This work was also financed by FEDER funds through the Competitivity Factors Operational Programme - COMPETE and by national funds through FCT within the scope of the projects POCI-01-0145-FEDER-007633 and POCI-01-0145-FEDER-016841 (IntegraCrete - PTDC/ECM-EST/1056/2014).

References

[1] Oliveira MA. A Multi–Physics Approach Applied to Masonry Structures with Non–Hydraulic Lime Mortars [PhD Theis]. Guimarães, Portugal: University of Minho; 2015.
[2] Oliveira MA, Azenha M, Lourenço PB. Simulation of Humidity Fields in Concrete: Experimental Validation and Parameter Estimation Journal of Advanced Concrete Technology - J-Stage. 2015;13:214-29.
[3] Azenha M. Numerical simulation of the structural behaviour of concrete since its early ages [PhD Thesis]: University of Porto, University of Tokyo.; 2009.
[4] Baroghel-Bouny V, Mainguy M, Lassabatere T, Coussy O. Characterization and identification of equilibrium and transfer moisture properties for ordinary and high-performance cementitious materials. Cement and Concrete Research. 1999;29(8):1225-38.
[5] Grasley ZC. Measuring and modeling the time-dependent response of cementitious materials to internal stresses: University of Illionois at Urbana-Champaign; 2006.
[6] Ferretti D, Bažant ZP. Stability of ancient masonry towers: Moisture diffusion, carbonation and size effect. Cement and Concrete Research. 2006;36(7):1379-88.
[7] Saetta AV, Vitaliani RV. Experimental investigation and numerical modeling of carbonation process in reinforced concrete structures: Part II. Practical applications. Cement and Concrete Research. 2005;35(5):958-67.
[8] Saetta AV, Vitaliani RV. Experimental investigation and numerical modeling of carbonation process in reinforced concrete structures: Part I: Theoretical formulation. Cement and Concrete Research. 2004;34(4):571-9.
[9] Saetta AV, Schrefler BA, Vitaliani RV. 2 – D model for carbonation and moisture/heat flow in porous materials. Cement and Concrete Research. 1995;25(8):1703-12.
[10] Saetta AV, Scotta RV, Vitaliani RV. Analysis of Chloride Diffusion into Partially Saturated Concrete. Materials Journal. 1993;90(5):441-51.
[11] Nehdi M, Hayek M. Behavior of blended cement mortars exposed to sulfate solutions cycling in relative humidity. Cement and Concrete Research. 2005;35(4):731-42.

[12] Jennings HM, Bullard JW, Thomas JJ, Andrade JE, Chen J. J., W SG. Characterization and modeling of pores and surfaces in cement paste: correlations to processing and properties. Journal of Advanced Concrete Technology - J-Stage. 2008;6(1):5-29.
[13] Zhang Z. Modelling of sorption hysteresis and its effect on moisture transport within cementitious materials. Paris: Paris Est , École Doctorale Sciences, Ingénierie et Environnement 2014.
[14] Bažant ZP, Najjar LJ. Drying of concrete as a nonlinear diffusion problem. Cement and Concrete Research. 1971;1(5):461-73.
[15] CEB–FIP. Model Code 1990. Comité Euro–International Du Béton; 1993. p. 437.
[16] CEB–FIP. Model Code 2010, V1. Comité Euro–International Du Béton; 2010. p. 318.
[17] Oliveira MA, Azenha M, Lourenço PB. Simulation of Humidity Fields in Concrete: Experimental Validation and Parameter Estimation Journal of Advanced Concrete Technology - J-Stage. 2015;13(4):214-29.
[18] Persson B. Moisture in concrete subjected to different kinds of curing. Materials and Structures. 1997;30(9):533-44.
[19] Kim J-K, Lee C-S. Moisture diffusion of concrete considering self-desiccation at early ages. Cement and Concrete Research. 1999;29(12):1921-7.
[20] Croft DRA, Lilley DG. Heat Transfer Calculations Using Finite Difference Equations. London: Applied Science Publishers LTD; 1977.
[21] Özisik MN. Heat conduction. 2nd edition ed: John Wiley & Sons; 1993.
[22] Kelley CT. Solving Nonlinear Equations with Newton's Method (Fundamentals of Algorithms): Society for Industrial and Applied Mathematics; 1987.
[23] TNO-DIANA-BV. Diana User´s Manual. Delft, The Netherlands: Release 9.4; 2010.
[24] Persson B. Hydration and strength of high performance concrete. Advanced Cement Based Materials. 1996;3(3–4):107-23.
[25] Persson B. Seven-Year Study on the Effect of Silica Fume in Concrete. Advanced Cement Based Materials. 1998;7(3–4):139-55.
[26] Zhi P, Xianyu J, Nanguo J. Theoretical Modeling of Concrete Moisture Diffusion Surface Factor. Earth and Space 2010: Engineering, Science, Construction,and Operations in Challenging Environments2010. p. 3610–6.
[27] Azenha M, Maekawa K, Ishida T, Faria R. Drying induced moisture losses from mortar to the environment. Part I: experimental research. Materials and Structures. 2007;40(8):801-11.
[28] Azenha M, Maekawa K, Ishida T, Faria R. Drying induced moisture losses from mortar to the environment. Part II: numerical implementation. Materials and Structures. 2007;40(8):813-25.